A Novel Fuel-Cell Electric Articulated Vehicle and Its Drop-and-Pull Transport System

Yanwei Liu [1], Zhenye Li [1], Yuzhong Chen [1] and Kegang Zhao [2,*]

[1] School of Electromechanical Engineering, Guangdong University of Technology, Guangzhou 510640, China; ywliu@gdut.edu.cn (Y.L.); zhenyel@foxmail.com (Z.L.); chen.yz.1996@foxmail.com (Y.C.)

[2] National Local Engineering Laboratory of Automobile Parts Technology, South China University of Technology, Guangzhou 510640, China

* Correspondence: kgzhao@scut.edu.cn; Tel.: +86-189-2512-3708

Abstract: Drop-and-pull transportation can repeatedly utilize tractors with different trailers and reduce costs, carbon emissions, and the number of tractors to purchase and use. Fuel-cell electric vehicles (FCEV) possess high power and long drive endurance. These performance characteristics complement the performance requirements of drop-and-pull transportation of heavy loads and long mileage. This paper proposes a novel fuel-cell electric articulated vehicle featuring three power sources: fuel cell, power battery, and ultracapacitor. Then, based on the proposed vehicle, we expound on a highly efficient and flexible transport system. To compare economics and durability of fuel-cell electric trailers with two energy sources (i.e., fuel-cell-battery) and three energy sources, we developed and simulated a rule-based energy management strategy under driving conditions. The results indicate that, although similar levels of fuel economy and capacity degradation of the fuel cell occur for the proposed vehicle and its two-energy-source counterpart, the ampere–hour throughput of three-energy-source vehicles was 64% lower than that of two-energy-source vehicles, which indicates the introduction of the ultracapacitor in fuel-cell-battery electric articulated vehicles can offer significant protection to the power battery. This result shows that the three energy sources increase the service life of the energy system.

Keywords: fuel cells; articulated vehicle; drop-and-pull transportation; energy management strategy

1. Introduction

Petroleum consumption has been continuously increasing owing to rapid social and economic developments worldwide. This growth has led to issues such as petroleum shortages and various types of environmental pollution. Meanwhile, vehicles powered by fuel cells do not cause pollution while achieving superior energy efficiency compared to conventional vehicles powered by fossil fuels. In addition, they only require a short hydrogen refueling time. Owing to these advantages, extensive use of fuel-cell vehicles can help reduce petroleum consumption and atmospheric pollution [1]. Hence, fuel-cell technology is an important factor contributing toward sustainable development in the automobile industry; it is also an ideal solution to global energy and environmental problems.

Drop-and-pull transportation is a new and efficient form of transport organization. In this paradigm, tractors can rapidly drop off trailers at the trailer exchange point, hang new trailers, or drive empty to perform the next task without waiting for loading and unloading, which improves transportation efficiency. Compared with traditional transportation methods, drop-and-pull transportation can repeatedly utilize tractors with different trailers and reduce costs, carbon emissions, and the number of tractors to purchase and use [2]. Numerous researchers have studied hybrid trailers with the objective of conserving energy and reducing emissions, but most of the studies are focused on

battery–engine hybrids [3–5]. Furthermore, research analysis shows that if the battery power is not derived from renewable energy, then hybrid trailers are not significantly different from traditional trailers in terms of emissions and life cycle [6].

Hydrogen fuel-cell vehicles possess strong adaptability to rapid load changes, high energy conversion efficiency, appropriate dynamic characteristics, low operating noise, and zero exhaust emissions [7]. These qualities perfectly satisfy the performance requirements (i.e., being able to transport heavy loads and travel long distances) of articulated vehicles, but research on the application of fuel cells to heavy commercial vehicles is relatively rare. Thus, this study proposes a novel, fuel-cell electric articulated vehicle featuring three power sources: fuel cells, power batteries, and ultracapacitors. During actual operation, power can be provided by a single source or by multiple power sources functioning simultaneously. This design enables a more flexible power output. Based on the proposed fuel-cell electric articulated vehicles and various facilities, such as freight storage areas, hydrogen stations, and charging stations, a highly efficient and flexible transport system comprising fuel-cell electric articulated vehicles was designed in this study. Moreover, energy management strategies based on different rules were formulated. Subsequently, a simulation accounting for actual driving conditions was conducted. The fuel economy and the durability of the fuel-cell electric articulated vehicles with three power sources were compared with those of their counterparts with two power sources.

2. Fuel-Cell Electric Articulated Vehicles and the Transport Systems

The fuel cell stack cannot efficiently respond to the sudden upward and downward powers required during acceleration and deceleration, respectively, nor can it effectively start the vehicle with the considerable initial power required. Furthermore, the fuel cell stack cannot store the regenerative power produced during deceleration and braking, thus an additional energy storage device is required [8]. Generally, the typical topology of an FCEV consists of at least two power sources—a fuel-cell system and an energy storage system, such as a lithium battery system or ultracapacitors. In an FCEV, the fuel cell is the main power source of the system, and the battery provides the supplementary energy required during FC start up and high load demand. Ultracapacitors are known to have a high dynamic operation and high efficiency. When an FCEV is equipped with double direct current (DC)-DC converters, ultracapacitors can satisfy the requirements of pulse load to ensure the power balance between demand and generation and to keep the system output voltage constant during operation [9]. In this way, the high efficiency and the environmental friendliness of fuel cells can be exploited while simultaneously utilizing the high energy densities of power batteries or the high power densities of ultracapacitors. This approach improves the performance of the power system, increases the service life of fuel cells, and enhances vehicle driving endurance through regenerative braking. Considering these benefits, this paper proposes a novel type of fuel-cell-ultracapacitor-power battery hybrid electric articulated vehicle (Figure 1). On this basis, a highly efficient and flexible drop-and-pull transport system comprising fuel-cell electric articulated vehicles was designed.

Drop-and-pull transport allows the articulated vehicles and trailers to have different types of power systems according to their own structures and operating methods. The energy system of the articulated vehicle consists of a fuel-cell-ultracapacitor hybrid electric system and a power battery system. The two systems can be coupled to provide output. Normally, when the vehicle is loaded, it is quite heavy. Hence, to meet the power demands due to heavy loading and uphill driving, the hybrid electric articulated vehicle must be equipped with batteries that can satisfy such high power demands. However, when the trailers are detached from the towing vehicle, lower power is sufficient. The power demand can be satisfied by the fuel-cell–ultracapacitor hybrid system alone. In addition, loaded trailers may exhibit freight safety issues (such as fires) during hydrogen refueling. Furthermore, when an articulated vehicle is equipped with batteries that can satisfy the high power demands, the batteries are often heavier. After considering these issues, in this study, we decided to install hydrogen tanks, hydrogen fuel cells, ultracapacitors, regenerative braking devices, energy management controllers, and whole-vehicle controllers onto the articulated vehicles (tractors), whereas the relatively heavy power

batteries are installed onto the trailers. The power batteries can be detached from or connected to the power system of the articulated vehicle as the trailers are unhooked from or hooked to the vehicles. Both the articulated vehicles and the trailers are driven independently by hub motors to realize multi-wheel distributed drive. Based on the differences in fuel and power levels, driving conditions, and remaining driving range, electricity to the articulated vehicles can be provided independently or simultaneously by fuel cells, ultracapacitors, and power batteries. As the transport routes and the travel times of the articulated vehicles can be restricted, the constraints caused by high investments in and wide distribution of hydrogen refueling infrastructure can be avoided. The drop-and-pull transportation method of one tractor with multiple trailers provides the possibility for tractors and trailers to carry different types of power systems according to the characteristics of their respective structures and operating methods. Based on the proposed novel fuel-cell composite energy source electric articulated vehicle, a fuel-cell electric trailer fleet is formed. Based on the traffic information network environment and the layout of the trailer fleet, this study also proposes a fuel-cell electric trailer transportation system.
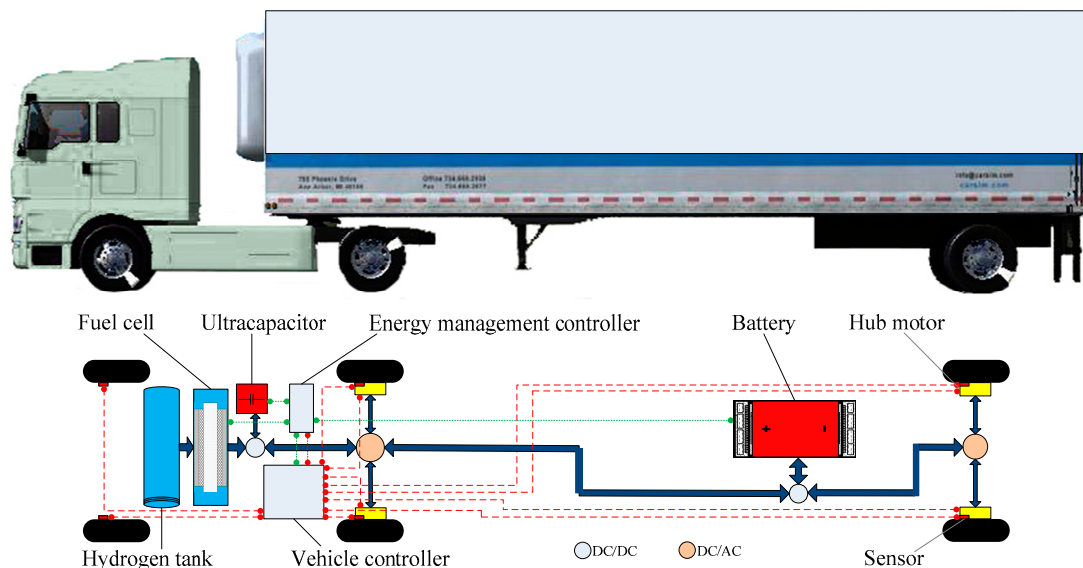

Figure 1. Configuration of components in the proposed fuel-cell electric articulated vehicle.

The proposed fuel-cell electric articulated vehicles can be refueled via hydrogen refueling of the vehicles or battery recharging or by exchanging the trailers, as the power batteries can be detached from or connected to the power systems of the articulated vehicles as the trailers are unhooked from or hooked to the vehicles. Considering that charging stations are available at the destinations, trailers that are no longer needed can be detached at the destinations for unloading and charging until the next articulated vehicle arrives. This can resolve the inability of vehicles to function when their power batteries are recharging. Hence, this approach can considerably enhance the efficiency of drop-and-pull transport. In addition, the articulated vehicles can tow ordinary trailers, and this feature enables wide applicability and high flexibility. Alternating the use of batteries can also extend their service life.

Sensors installed near the wheels of the articulated vehicles and trailers transmit vehicle motion information to the vehicle controllers. The vehicle controllers consequently adjust the motor speeds of the articulated vehicles and trailers according to the demands. Such information is then sent to the energy management controllers. Then, the energy management controllers control the power output of ultracapacitors, fuel cells, and power batteries to fulfil the power demands required by the operating conditions. Furthermore, all drive wheels of the articulated vehicles and trailers are independently driven by hub motors. Hence, the vehicles can be driven by four independent drive wheels. In addition, regenerative braking becomes possible for the vehicles. Considering factors such

as road, loading, and weather conditions, power allocation between multiple drive wheels can be adjusted by the vehicle controllers. Handling stability is then enhanced. In addition, by controlling the differential torques between the left and the right wheels, differential steering of multiple wheels can be realized [10]. Thus, the flexibility of the vehicles during U-turn maneuvers at low speeds and the handling stability during turning are increased. Under conditions where vehicle speed is reduced by braking, regenerative braking energy charges the ultracapacitors and power batteries. In addition, when high power output is required or significant changes occur in loading conditions, the ultracapacitors and the power batteries can provide most of the power needed, while the fuel cells need only to provide constant power output. This helps increase the service life of the fuel cells.

Drop-and-pull transport systems feature fixed freight storage areas. Hence, unlike the routes of ordinary passenger vehicles, those of drop-and-pull transport vehicles are restricted to connect various freight storage areas. In this study, the proposed transport system comprising the fuel-cell electric articulated vehicles was organized according to the following principles: connecting multiple destinations through a single route and hooking and unhooking along this route. As illustrated in Figure 2, an articulated vehicle departs from node A. Along its route, it undergoes sorting and reorganization of the freight one or more times in one or more freight storage areas. Finally, it arrives at node B. This process is repeated when it travels back from B to A.
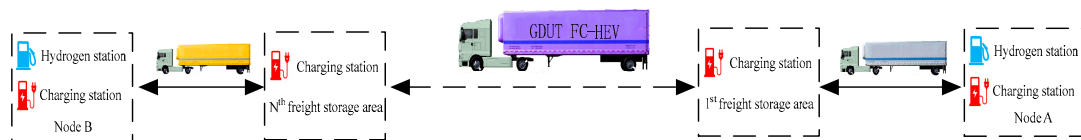
Figure 2. Transport mode connecting multiple destinations through one route.

This mode can be applied for cross-region less-than-truckload shipping, express delivery, and cross-border e-commerce logistics. Furthermore, convoys of the fuel-cell electric vehicles can be realized. Fuel-cell electric articulated vehicles in drop-and-pull transport systems can ignore the order of the freight storage areas (from the 1st to the Nth) and go past all of them. The freight storage areas at which the vehicle should stop are determined according to freight sorting information, traffic, road information, distributions of hydrogen and charging stations in the freight storage areas, configuration of the convoy, and hydrogen and battery power levels of the vehicle.

The proposed transport system combines fuel-cell electric articulated vehicles with a transport mode that connects multiple destinations through a single route. Because the fuel-cell electric articulated vehicles are relatively flexible in terms of energy supplies and convoy scheduling, additional hydrogen stations are required only in some highway rest areas and some freight storage areas, whereas additional charging stations are constructed in some freight storage areas. Thus, the demand for energy supplies by large-scale drop-and-pull transport is readily satisfied by the proposed transport system. A large-scale demonstration operation can be realized with a minor investment in infrastructure. Based on big data and vehicle networking technology, data collected from the fuel-cell electric vehicles, the distributions of charging and hydrogen stations in the system, and the global positioning system and the intelligent transportation system are integrated and processed in real time. Using information on road conditions, distributions of freight storage areas, freight, distribution of charging and hydrogen stations, vehicle energy conditions (i.e., battery power and hydrogen levels), and cost of the drop-and-pull transport system, average speeds, remaining range, remaining travel time, road elevations, and real-time traffic information along the routes can be calculated and predicted. This enables advance scheduling of the convoys of fuel-cell electric vehicles.

The tractor can tow a trailer equipped with a power battery system or a general trailer, which has a wide range of adaptability. In Figure 3, part of the drop-and-pull transport journey shown in Figure 2 is illustrated, assuming that a long-distance articulated vehicle travels 1000 km per day.
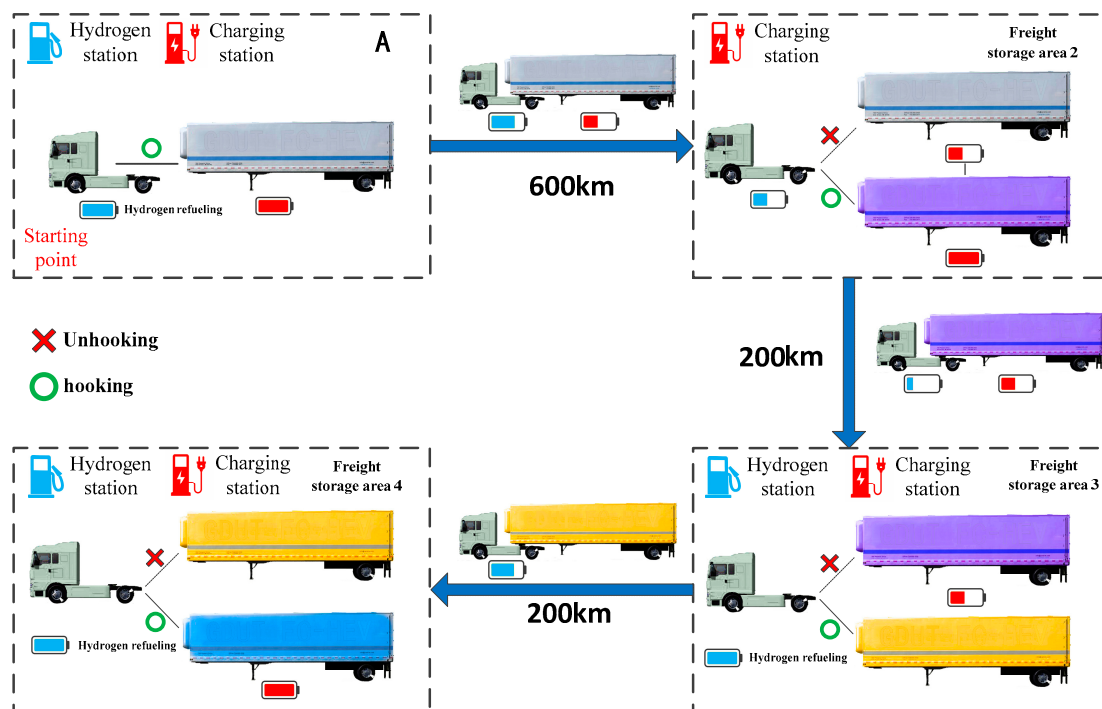
Figure 3. Drop-and-pull transport using fuel-cell electric articulated vehicles.

As shown in Figure 3, the loaded fuel-cell electric articulated vehicle departs from starting point A with a full hydrogen tank and fully charged power battery. During transport, according to hydrogen and battery power levels as well as the convoy configuration information, all the freight is delivered to freight storage area 2, which is 600 km from A, for sorting. This allows the vehicle to skip freight storage area 1 to ensure that battery power and time budget of the vehicle can be completely utilized. As freight storage area 2 has charging stations but no hydrogen stations, new trailers with fully charged batteries and sorted freight can be hooked to the articulated vehicle in the storage area. Then, the vehicle can depart and travel to the next freight storage area. Meanwhile, freight bound for freight storage area 1 can be transported from freight storage area 2 to freight storage area 1 with the help of other articulated vehicles in the convoy when they return to freight storage area 2. For the remaining journey, when the hydrogen level becomes too low, the vehicle can be refueled at a hydrogen station in a highway rest area or in a freight storage area equipped with hydrogen stations according to the distribution information of hydrogen stations. As shown in Figure 3, after the electric vehicle leaves freight storage area 2, it travels 200 km and arrives at freight storage area 3 for hydrogen refueling. In addition, in this freight storage area, freight sorting has been completed for some trailers, and these trailers must be transported. Hence, while the vehicle is being refueled, its trailers are replaced by ordinary trailers with sorted freight. Subsequently, it delivers the freight to freight storage area 4. Other organization schemes are possible, according to information such as hydrogen and battery power levels and freight of the vehicles, distributions of hydrogen and charging stations, and different types of traffic information. This allows highly flexible scheduling in the transport system using the fuel-cell electric vehicles.

Low-carbon, environmentally friendly, efficient, and highly unified transport of freight can be realized by deploying the proposed transport system using the proposed fuel-cell electric articulated vehicles with the help of traffic information. The system can be operated on a large scale over an extensive area with little investment in infrastructure. It provides significant economic and social benefits and thus has a high application potential.

3. Construction of the Numerical Model

The energy system model of the novel fuel-cell electric articulated vehicle consists mainly of a dynamic model of the fuel cell, a power battery model, and an ultracapacitor model. For the performance of the articulated vehicle, this study focused primarily on the fuel economy and the durability of the system.

3.1. Dynamic Model of the Energy System

3.1.1. Dynamic Model of the Fuel Cell

To describe the output characteristics of the fuel cell as well as the material transfer and the reaction inside the stack, researchers have proposed various mathematical models to fully describe the fuel cell [11–14]. The electrochemical model can not only describe the output characteristics of the battery but can also explain the specific relationship between the output characteristics and specific parameters such as temperature, pressure, and flow rate. Electrochemical models are the most widely used [14–18]. The fuel cell model employed is illustrated as an electrochemical model in this paper.

When liquid water is produced from the reactions in a proton exchange membrane fuel cell (PEMFC), the cell has an ideal standard potential of 1.229 V [14]. Because of irreversible losses, the actual potential of the cell decreases as the equilibrium potential declines. The actual irreversible loss of the cell is often known as polarization overpotential or overvoltage. The voltage loss that causes the open-circuit voltage of a PEMFC to drop can be divided into three types: activation polarization voltage loss, ohmic polarization voltage loss, and concentration polarization voltage loss [15].

The output voltage of a single PEMFC can be expressed as

$$E_{\text{cell}} = E_{\text{Nernst}} - U_{\text{act}} - U_{\text{ohm}} - U_{\text{co}}, \tag{1}$$

where E_{Nernst} denotes the thermal electromotive force, U_{act} is the activation polarization voltage loss, U_{ohm} is the ohmic polarization voltage loss, and U_{co} denotes the concentration polarization voltage loss.

The thermal electromotive force [16] is calculated by

$$E_{\text{Nernst}} = \frac{\Delta G}{2F} + \frac{\Delta S}{2F} \times (T - T_{\text{ref}}) + \frac{RT}{2F} \times \left(\ln\left(P_{\text{H}_2}\right) + 0.5\ln\left(P_{\text{O}_2}\right) \right), \tag{2}$$

where ΔG denotes the change in the Gibbs free energy, F is the Faraday constant, ΔS denotes the change in the entropy, R is the gas constant, P_{H_2} is the partial pressure of hydrogen at the anode catalyst-gas interface, P_{O_2} is the partial pressure of oxygen at the cathode catalyst-gas interface, T is the cell temperature, and T_{ref} denotes the reference temperature. By substituting ΔG, ΔS, and T_{ref} at standard atmospheric pressure and room temperature into Equation (2), the following simplified expression can be obtained:

$$E_{\text{Nernst}} = 1.229 - 8.5 \times 10^{-4} \times (T - 298.15) + 4.308 \times 10^{-5} \times T \times \left(\ln\left(P_{\text{H}_2}\right) + 0.5\ln\left(P_{\text{O}_2}\right) \right). \tag{3}$$

The activation polarization voltage loss can be expressed by

$$U_{\text{act}} = \xi_1 + \xi_2 \times T + \xi_3 \times T \times \ln\left(C_{\text{O}_2}\right) + \xi_4 \times T \times \ln(I), \tag{4}$$

where I denotes the current of the PEMFC. ξ_1, ξ_2, ξ_3, and ξ_4 are the empirical parameters; their values depend on the theoretical balance among kinetics, thermodynamics, and electrochemistry. C_{O_2} is the oxygen concentration at the cathode catalyst-gas interface, and C_{O_2} is a function of the cell temperature; according to Henry's law, it can be expressed as follows:

$$C_{\text{O}_2} = \frac{P_{\text{O}_2}}{5.08 \times 10^6 \times \exp(-498/T)}. \tag{5}$$

The ohmic polarization voltage loss [17] is expressed by

$$U_{ohm} = I \times R_{ohm} = I \times (R_m + R_c),$$ (6)

where R_m is the equivalent membrane resistance of the proton exchange membrane and R_c is the membrane resistance to the proton flow:

$$R_m = \frac{r_M \times l}{A},$$ (7)

$$r_M = \frac{181.6 \times \left(1 + 0.03J + 0.062 \times \left(\frac{T}{303}\right)^2 \times J^{2.5}\right)}{(\lambda - 0.634 - 3J) \times \exp\left(4.18 \times \left(\frac{T-303}{T}\right)\right)}.$$ (8)

The concentration polarization voltage loss is expressed by

$$U_{con} = -B \times \ln\left(1 - \frac{J}{J_{max}}\right),$$ (9)

where B is a constant determined by the battery type and the working condition, J is the actual current density (A/cm^2), which is equal to $\frac{I}{A}$, and J_{max} denotes the maximum current density. As temperature control is not our main focus in this article, we set the temperature to room temperature in order to simplify the calculation. The parameters of the fuel cell in Table 1 were obtained from an existing publication [18].

Table 1. Parameters of the fuel-cell model.

Parameter	Value	Parameter	Value
Number of single batteries N	1100	Curve fitting coefficient ξ_1	−0.9514
Working temperature of the fuel-cell stack T (K)	323	Curve fitting coefficient ξ_2	0.00312
Partial pressure of hydrogen P_{H2} (atm)	0.5	Curve fitting coefficient ξ_3	7.4×10^{-5}
Partial pressure of oxygen P_{O2} (atm)	0.5	Curve fitting coefficient ξ_4	1.87×10^{-4}
Gibbs free energy change ΔG (J/mol)	237,180	Proton exchange membrane thickness l (μm)	20
Activation area A (cm^2)	150	Membrane water content λ	20
Standard molar entropy change ΔS (J/mol)	−163.15	Fuel cell performance coefficient B	0.016
Reference temperature T_{ref} (K)	298.15	Equivalent capacitance C (F)	2.5
Faraday constant F (C/mol)	96486.7	Maximum current density J_{max} (A/cm^2)	1.5
Gas constant R (J/(Kmol))	8.314	Equivalent contact resistance of the membrane R_c (Ω)	3×10^{-4}

3.1.2. Power Battery Model

The single-battery model employed is as illustrated by the internal resistance model in Figure 4.
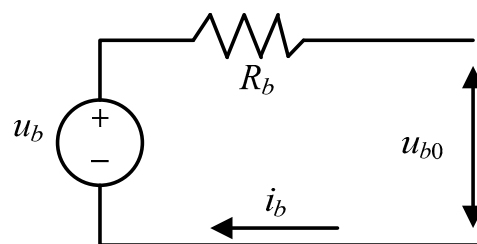
Figure 4. Equivalent model of the single-battery model [19].

The battery state of charge (BSOC) is obtained through ampere–hour integration [20]:

$$BSOC(t) = BSOC(t_0) - \frac{\int i_b(t)\mathrm{d}t}{Q_b},$$ (10)

where $BSOC(t_0)$ is the initial BSOC and Q_b is the battery capacity.

The battery power is calculated by

$$\begin{cases} u_{b0} = u_b \times (BSOC(t)) - i_b(t) * R_b(BSOC(t)) \\ P_{b,out}(t) = i_b(t) \times u_{b0} \end{cases}.$$ (11)

when $P_{b,out}$ is positive, the battery is discharging, and when $P_{b,out}$ is negative, the battery is charging. According to our experimental results, the open-circuit voltage u_b has a nonlinear relationship with the BSOC, as illustrated in Figure 5. In addition, the internal resistance R_b is related to the charging and discharging of the battery (Figure 6) [19].
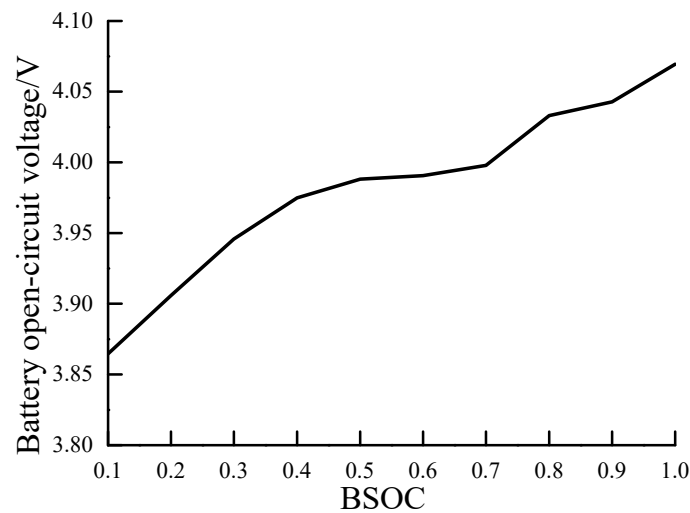

Figure 5. Relationship between open-circuit voltage and battery state of charge (BSOC) [19].
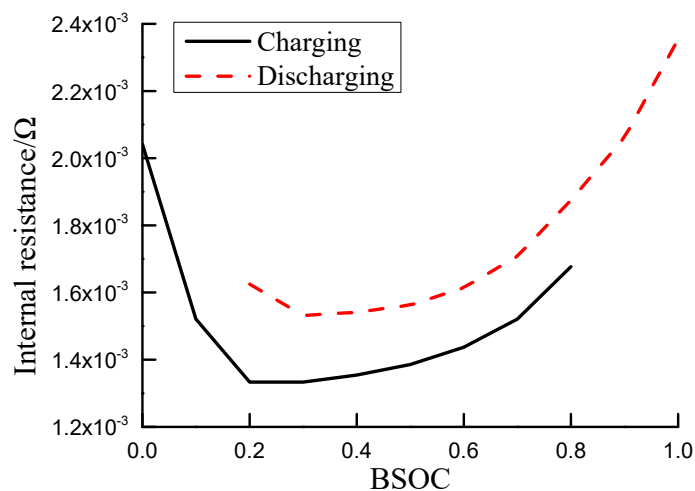

Figure 6. Relationship between internal resistance and BSOC during charging and discharging of the battery [19].

3.1.3. Ultracapacitor Model

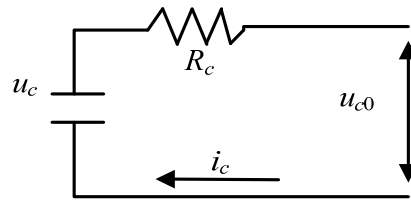The single-ultracapacitor model is illustrated in Figure 7.

Figure 7. Equivalent-circuit model of a single ultracapacitor [19].

In Figure 7, u_c denotes the open-circuit voltage of the ultracapacitor, u_{c0} is the terminal voltage, i_c denotes the current (positive during discharging, negative during charging), and R_c represents the equivalent series internal resistance. The equation for calculating the ultracapacitor state of charge (USOC) is as follows [21]:

$$USOC(t) = USOC(t_0) - \frac{\int i_c(t)\mathrm{d}t}{C_c \times u_{cmax}},$$ (12)

where $USOC(t_0)$ is the initial USOC, C_c denotes the capacitance of the ultracapacitor, and u_{cmax} is the maximum voltage.

The power of the ultracapacitor is

$$\begin{cases} u_{c0} = u_c \times (USOC(t)) - i_c(t) * R_c \\ \quad P_{c,out}(t) = i_c(t) \times u_{c0} \end{cases}.$$ (13)

A positive $P_{c,out}$ indicates that the ultracapacitor is discharging, whereas a negative value indicates charging of the ultracapacitor. As the open-circuit voltage u_c varies linearly with the USOC, the energy of the ultracapacitor E_c is expressed as [22]

$$\begin{cases} USOC(t) = \frac{u_c(t)}{u_{cmax}} \\ E_c = 0.5 \times C_c \times u_{cmax}^2 \times USOC^2(t) \end{cases}.$$ (14)

3.2. Fuel Economy and Durability Model

3.2.1. Fuel Economy of the Fuel-Cell Articulated Vehicle System

The fuel economy of the proposed fuel-cell articulated vehicle system is evaluated on the basis of the total equivalent hydrogen consumption during operation. The instantaneous power consumption from the battery and the ultracapacitor can be equal to the chemical energy from the fuel. The instantaneous hydrogen consumption is composed of direct hydrogen consumption by the fuel-cell system and indirect equivalent hydrogen consumption by the battery and the ultracapacitor [23].

The hydrogen consumption by the fuel cell C_1 [24] is

$$C_1 = \frac{1}{2F} \int_0^T M_{H_2} \times I_{fc}\mathrm{d}t,$$ (15)

where M_{H_2} is the molar mass of hydrogen, F is the Faraday constant, and I_{fc} is the current of the fuel cell.

Our computation here is based on the equation in [25], but to simplify the calculation, we converted the integral power operation in the study into the energy solution. Thus, the equivalent hydrogen consumption by the power battery and ultracapacitor is defined as C_2.

$$C_2 = \frac{1}{J_{H2}} \times \left(\frac{E_{bat} \times \Delta SOC_{bat}}{\overline{\eta_{fc}} \times \overline{\eta_{bat}} \times \overline{\eta_{DC/DC}}} + \frac{E_{cap} \times \Delta SOC_{cap}}{\overline{\eta_{fc}} \times \overline{\eta_{cap}} \times \overline{\eta_{DC/DC}}} \right), \tag{16}$$

where $\overline{\eta_{fc}}$ and $\overline{\eta_{bat}}$ are the average efficiency of the fuel cell and the average charging efficiency of the power battery, respectively; $\overline{\eta_{cap}}$ and $\overline{\eta_{DC/DC}}$ are the average charging efficiency of the ultracapacitor and the efficiency of the DC-DC converter, respectively. E_{bat} and E_{cap} are the amounts of energy stored in the power battery and the ultracapacitor, respectively, and J_{H2} is the calorific value of hydrogen. Hence, the fuel economy can be expressed by

$$C = C_1 + C_2 = \frac{1}{2F} \times \int_0^T M_{H_2} \times I_{fc} dt + \frac{1}{J_{H2}} \times \left(\frac{E_{bat} \times \Delta SOC_{bat}}{\overline{\eta_{fc}} \times \overline{\eta_{bat}} \times \overline{\eta_{DC/DC}}} + \frac{E_{cap} \times \Delta SOC_{cap}}{\overline{\eta_{fc}} \times \overline{\eta_{cap}} \times \overline{\eta_{DC/DC}}} \right). \tag{17}$$

3.2.2. Durability of the Fuel-Cell Articulated Vehicle System

Ultracapacitors have high power densities, rapid charging and discharging rates, and a significantly longer cycle life than those of power batteries and fuel cells; they can typically complete 10^6 cycles. Hence, when the durability of the system is assessed, the durability of the fuel cell and the power battery is the dominant factor.

External factors affecting the service life of the power battery of a vehicle include operating temperature, depth of discharge, and charging–discharging rates. The service life factor of a power battery under the influence of charging and discharging is defined as the effective ampere–hour throughput (Aheff). To avoid high-current discharging of the battery, the penalty factor σ is introduced in the calculation of Aheff [26].

$$\begin{cases} Aheff(t) = \int_0^{t_f} \sigma(t) \times |i_b(t)| dt \\ \sigma(t) = \frac{1.6}{625} \times i_c^2(t) + 1 \\ i_c(t) = \frac{i_b(t)}{Q_b} \end{cases}, \tag{18}$$

where σ is the penalty factor. It is determined mainly by charging–discharging rate i_c, temperature, and depth of discharge.

The service life of the fuel cell is closely related to its operating conditions. Current research suggests that the operating conditions causing fuel-cell performance degradation are the number of start–stop cycles, duration of load variation, idle time, and duration of high-power operation [27]. The capacity degradation of the fuel cell $\Delta \varnothing FC_{degrad}$ is calculated as

$$\Delta \varnothing FC_{degrad} = Kp \times ((k_1 \times t_1 + k_2 \times n_1 + k_3 \times t_2 + k_4 \times t_3) + \beta), \tag{19}$$

where β is the rate of natural degradation; t_1, n_1, t_2, and t_3 are idle time, number of start–stop cycles, duration of significant load variation, and duration of high-power operation, respectively; k_1, k_2, k_3, and k_4 are the degradation coefficients due to idle running, start–stop, significant load variation, and high-power operation, respectively. Further, Kp is the correction coefficient. Table 2 lists the values of the coefficients in Equation (19), as obtained from [28].

Table 2. Values of the coefficients in Equation (19).

Coefficient	Value	Definition
k_1	0.00126 (%/h)	Power output is less than 5% of the maximum power
k_2	0.00196 (%/cycle)	One complete start–stop cycle
k_3	0.0000593 (%/h)	Absolute value of the load variation per second exceeds 10% of the maximum power
k_4	0.00147 (%/h)	Power output is greater than 90% of the maximum power
Kp	1.47	the correction coefficient
β	0.01 (%/h)	Rate of natural degradation

4. Simulation and Results Analysis

### 4.1. Construction of the Simulation Model

The proposed vehicle is a fuel-cell-ultracapacitor-power battery hybrid electric articulated vehicle. To produce a highly dynamic and economical articulated vehicle, reasonable energy management strategies are required. This enables effective coordination among the fuel cell, the ultracapacitor, and the power battery and enables designers to take full advantage of these energy sources. Most of the research results from the past few decades can be divided into three categories of energy management strategies: rule-based strategies, optimization-based strategies [29], and learning-based energy management strategies [30]. The rule-based energy management strategy is widely applied, because the method is easy to implement, has high computational efficiency, and is quickly verifiable by experiments [31–33]. In this study, the integrated ultracapacitor-power battery hybrid system was treated as a power source that acts as a secondary energy source to regulate the power output by the fuel cell. Subsequently, energy management strategies based on rules were established to manage the energy provided by the fuel cell and the hybrid power system. The fuel cell, the ultracapacitor, and the power battery are controlled independently according to their power output characteristics. Thus, coordinated control of these energy sources can be realized, using which a novel fuel-cell electric articulated vehicle with high fuel economy and system durability was designed. In addition, fuel economy and system durability of the proposed fuel-cell electric articulated vehicle were compared with those of a fuel-cell-power battery hybrid articulated vehicle.

Relatively significant degradation of the fuel-cell service life is caused by low- and high-power operation, considerable load variations, and several start–stop cycles. Hence, after starting, stable output from the fuel cell should be maintained whenever possible. Moreover, the ultracapacitor-power battery hybrid system should dynamically provide the required additional power according to dynamic power demands. This increases the service life of the fuel cell. Moreover, the ultracapacitor plays a crucial role in providing instantaneous power, especially in acceleration and regenerative braking. In fact, compared with battery and fuel cell, its power density, durability, and efficiency in charge-discharge cycles provide more advantages [34]. Thus, its properties should be completely utilized in the ultracapacitor-power battery hybrid system to avoid high-current charging and discharging of the power battery. The service life of the power battery can thereby be extended. Hence, the regenerative braking energy should be stored by the ultracapacitor as much as possible. Only the excess energy should be used to charge the power battery. Furthermore, when the power demand for the secondary energy source is high, high power output is provided by the ultracapacitor, whereas supplementary power is provided by the power battery. Therefore, to further increase the cycle life of the fuel cell and the power battery and to enhance the whole-vehicle fuel economy, the rules for energy management in this study were defined as follows:

1. When the power demand exceeds the average demand power of the working conditions, the fuel cell is initialized. Thereafter, the output power of the fuel cell should be maintained at relatively stable to maximize the service life of the cell. In order to maintain a relatively stable output of fuel cell, Butterworth low-pass filter is applied to the demand power of the working conditions. Additionally, we set the output power of fuel cell to be equal to the filtered demanded power.

When the power demand of the working conditions is smaller than the output from the fuel cell, the excess is used to charge the hybrid system. When the power demand of the working conditions is higher than the fuel cell output, the hybrid system compensates for this difference.

2. The difference between the whole-vehicle power demand and the power provided by the fuel cell is the hybrid system power demand. When this hybrid system power demand is greater than zero, the USOC is first determined. If the USOC is lower than its lower limit (0.4), the power battery must provide the entire amount of power required. However, if the USOC is higher than 0.4, the hybrid system power demand is compared to its average counterpart. According to the analysis of the power demand of the working conditions and based on the requirement to completely utilize the ultracapacitor and extend the service life of the power battery, if the hybrid system power demand is greater than the average hybrid power demand, the power battery is responsible for 2/5 of the demand, and the ultracapacitor must provide the remainder. Conversely, if the hybrid system power demand is lower than the average hybrid power demand, the ultracapacitor must provide the entire amount of power required.

3. When the hybrid system power demand is less than zero, the USOC is first determined. If it exceeds its upper limit (0.8), all the power is used to charge the power battery. Otherwise, all the power is used to charge the ultracapacitor.

In Figures 8 and 9, $P_{\text{low-pass\_req}}$ is the power demand of the working conditions after Butterworth low-pass filtering, P_{fc} is the power output of the fuel cells, P_{bat} is the power output of the batteries, P_{cap} is the power output of the ultracapacitors, P_{req} is the power demand of the working conditions, $P_{\text{bat\_cap}}$ is the hybrid system power demand (the power of the battery and ultracapacitor, $P_{\text{bat\_cap}} = P_{\text{req}} - P_{\text{fc}}$), and $P_{\text{avg\_bat\_cap}}$ is the average hybrid power demand.
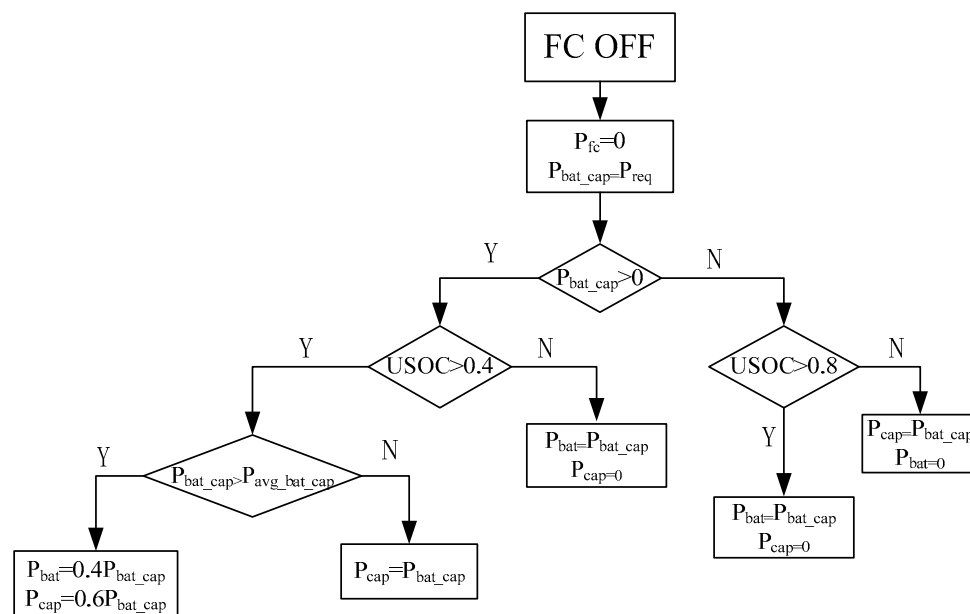
Figure 8. Flowchart of rules for energy management when the fuel cell is off.

In this study, the C-WTCV working conditions of heavy commercial vehicles were adopted as the working conditions of the proposed fuel-cell electric articulated vehicle for simulation. According to the power demand of the C-WTCV working conditions of heavy commercial vehicles and corresponding driving indexes, we referred to the parameter matching methods in [26,34,35] to match the parameters of motor, fuel cell, battery, and ultracapacitor. The parameters used in the simulation are listed in Tables 3–7.
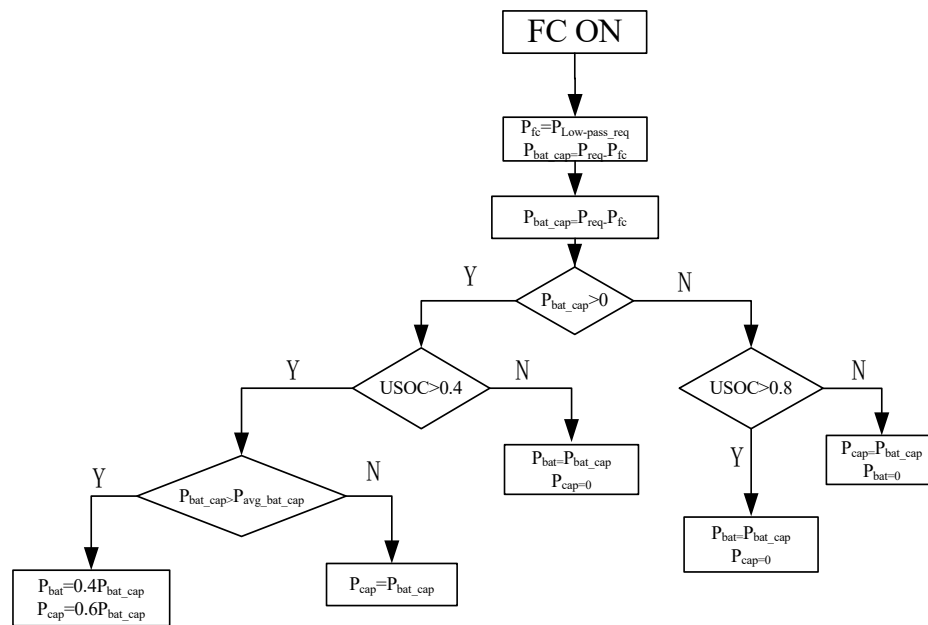
Figure 9. Flowchart of rules for energy management when the fuel cell is on.

Table 3. Whole-vehicle parameters.

Parameter	Value	Parameter	Value
Length (mm)	6130	Width (mm)	2495
Height (mm)	2960	Whole-vehicle curb weight (kg)	5900
Total weight (kg)	18	Rolling resistance coefficient	0.02
Air resistance coefficient	0.7	Frontal area (m^2)	7.4
Rolling radius (m)	0.512	Final drive ratio	4.875
Trailer weight (kg)	4900	-	-

Table 4. Motor parameters.

Parameter	Value	Parameter	Value
Peak power (kW)	380	Rated power (kW)	190
Peak torque (Nm)	6600	Rated torque (Nm)	3300
Peak speed (r/m)	2600	Rated speed (r/m)	1100
Rated voltage (V)	408	Efficiency	0.92

Table 5. Fuel cell parameters.

Parameter	Value	Parameter	Value
Peak power (kW)	130	Rated power (kW)	80
DC/DC efficiency	0.94	-	-

Table 6. Power battery parameters.

| Parameter	Value	Parameter	Value
Nominal voltage (V)	3.6	Single-battery capacity	37 Ah
Number of batteries in series	113	Number of batteries in parallel	2
BSOCmin	0.4	BSOCmax	0.8

Table 7. Ultracapacitor parameters.

Parameter	Value	Parameter	Value
Capacitance (F)	3000	Maximum voltage (V)	2.7
Internal resistance (Ω)	0.00029	Number of ultracapacitors in series	76
Number of ultracapacitors in parallel	5	USOCmin	0.25
USOCmax	0.9	-	-

DC: direct current; USOC: ultracapacitor state of charge.

4.2. Analysis of Simulation Results

A simulation was conducted using MATLAB on the basis of the aforementioned energy management rules under the C-WTCV working conditions. Figure 10 shows the relationships between the power demand and the power output by the three energy sources under the C-WTCV working conditions. In Figures 10 and 11, P_{req} is the power demand of C-WTCV.
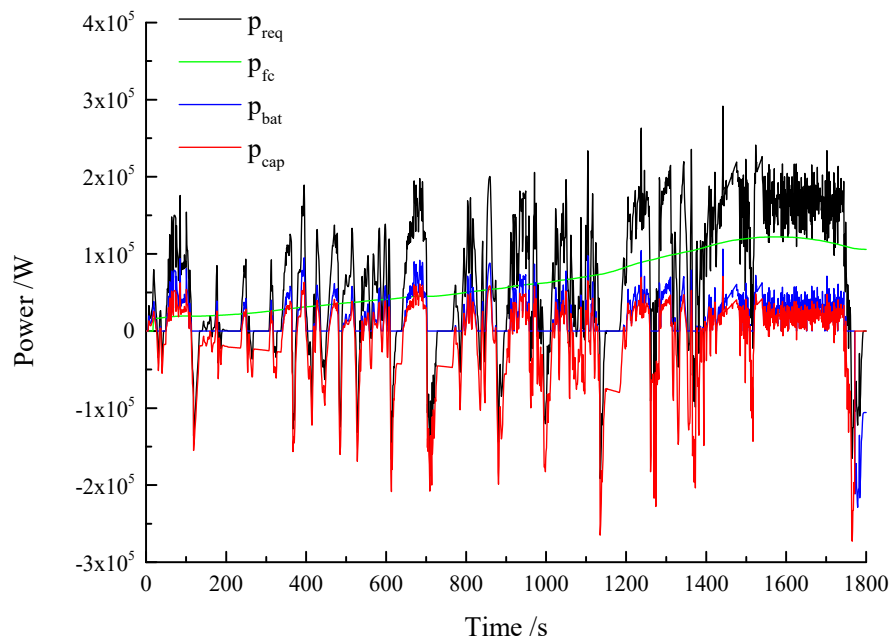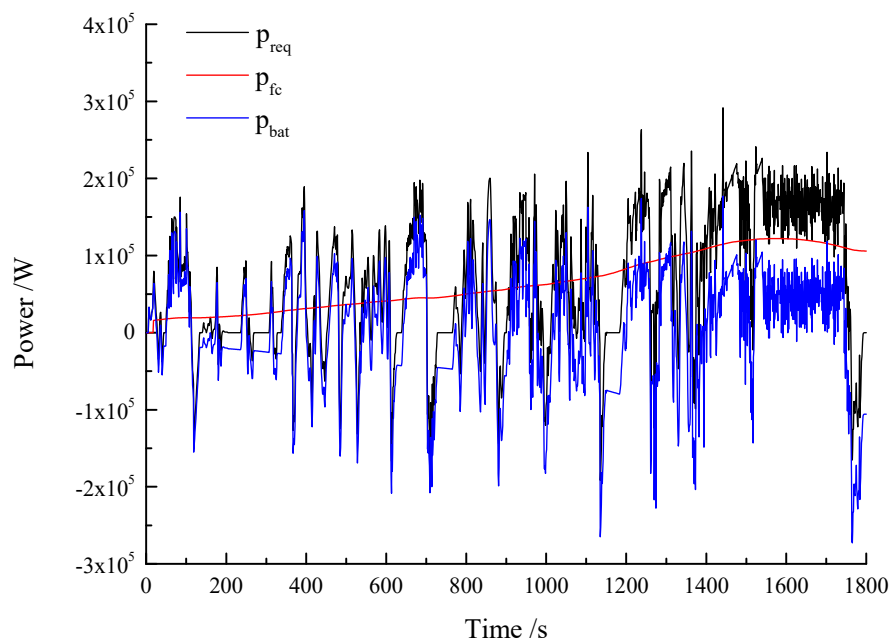

Figure 10. Relationships between power output and power demand by the three energy sources.

Figure 11 illustrates the relationships between the power demand and the power output by the two energy sources of the fuel cell-power battery hybrid electric articulated vehicles under the C-WTCV working conditions.

The simulation results demonstrate that the fuel cell was providing relatively stable output after it was switched on. When the power demand was smaller than the output by the cell, the excess power was used to charge the power battery and the ultracapacitor. Conversely, when the power demand was greater than the fuel cell output, the power battery and the ultracapacitor compensated for the difference. For the articulated vehicle with two energy sources, when the demand was smaller than the output by the fuel cell, all the excess power was used to charge the power battery. When the demand was greater than the fuel cell output, the difference was supplied by the power battery.

From the simulation results, the fuel economy and the durability of the systems were calculated. The equivalent hydrogen consumption by the proposed articulated vehicle with three energy sources was 4443.6 g for a C-WTVC cycle. The capacity degradation of the fuel cell was 0.0074%, and the ampere–hour throughput of the power battery was 0.6401 Ah. Under the same working conditions, the equivalent hydrogen consumption by an articulated vehicle with two energy sources (i.e., fuel cells

and batteries) was 4436.2 g. The capacity degradation of the fuel cell was 0.0074%, and the ampere–hour throughput of the power battery was 1.7891 Ah. From the simulation results, although similar levels of fuel economy and capacity degradation of the fuel cell are noted for the proposed vehicle and its counterpart equipped with two energy sources, the ampere–hour throughput of the vehicle with two energy sources was higher than the vehicle with three energy sources. The ampere–hour throughput of the vehicle with three energy sources was 64% lower than that of the vehicle with only two energy sources for a C-WTVC cycle. This indicates that the introduction of the ultracapacitor in the fuel-cell-battery articulated vehicle can offer significant protection for the power battery. Ultracapacitors have a significantly longer cycle life than those of power batteries and fuel cells, and thus when the fuel cell life is similar, the extension of the battery life will extend the service life of the energy system.

Figure 11. Relationships between power output and power demand by two energy sources.

5. Conclusions

Fuel cells are known for their high power output and rapid refueling property, and ultracapacitors and power batteries have high power density and high energy density, respectively. This study innovatively integrated these advantages to design a novel fuel-cell-ultracapacitor-power battery hybrid electric articulated vehicle. By using this vehicle, convoys of fuel-cell electric articulated vehicles can be realized. A drop-and-pull transport system of these vehicles was proposed by effectively combining the advantages of the vehicles (having multiple modes of energy supply and allocation, allowing the vehicles to be driven with these various combinations and allowing replacement of batteries) with the features of drop-and-pull transport. Moreover, energy management strategies based on some rules were established to conduct simulation analysis. The simulation results for the proposed articulated vehicles were compared with those for the fuel-cell electric articulated vehicles with two energy sources. It was found that the use of the fuel-cell electric articulated vehicles with three energy sources can further extend the service life of the system. The proposed drop-and-pull transport system using the new fuel-cell electric articulated vehicles is more flexible because of its mode of organization and transport scheme. In addition, large-scale demonstrative operation over a large area can be realized with small infrastructure investment. It provides significant economic and social benefits and thus has a high application potential.

This paper describes a prototype for a novel drop-and-pull transport system comprising a new type of fuel-cell electric articulated vehicles. Future studies should integrate different types of resources, for example, various types of detailed traffic information, more effective energy management strategies, and distributions of different types of infrastructure. Another research direction is to apply the proposed system to more complex drop-and-pull transport systems. The proposed system still has room for improvement, but it also shows great potential. The findings of this study offer important insights into the development of transport systems using renewable energy.

Author Contributions: Conceptualization, Y.L.; methodology, Z.L. and Y.C.; investigation, Y.L., Z.L., Y.C. and K.Z.; formal analysis, Y.L., Z.L., Y.C. and K.Z.; writing—original draft, Z.L.; writing—review & editing, K.Z. and Y.L.; All authors have read and agreed to the published version of the manuscript.

Conflicts of Interest: The authors declare no conflict of interest.

References

1. Kasimalla, V.K.; Naga, S.G.; Velisala, V. A review on energy allocation of fuel cell/battery/ultracapacitor for hybrid electric vehicles. *Int. J. Energy Res.* **2018**, *42*, 4263–4283. [CrossRef]
2. Yang, Z.; Yang, G.; Xu, Q.; Guo, S.; Jin, Z. Optimization on tractor-and-trailer transportation scheduling with uncertain empty-trailer tasks. *J. Traffic Transp. Eng.* **2016**, *16*, 103–111.
3. Fries, M.; Kruttschnitt, M.; Lienkamp, M. Operational strategy of hybrid heavy-duty trucks by utilizing a genetic algorithm to optimize the fuel economy multi objective criteria. *IEEE Trans. Ind. Appl.* **2018**, *54*, 3668–3675. [CrossRef]
4. Lhomme, M.; Bouscayrol, A.; Syed, S.A.; Roy, S.; Gailly, F.; Pape, O. Energy savings of a hybrid truck using a ravigneaux gear train. *IEEE Trans. Veh. Technol.* **2017**, *66*, 8682–8692. [CrossRef]
5. Pham, T.H.; Kessels, J.T.B.A.; Van den Bosch, P.P.J.; Huisman, R.G.M. Analytical solution to energy management guaranteeing battery life for hybrid trucks. *IEEE Trans. Veh. Technol.* **2016**, *65*, 7956–7971. [CrossRef]
6. Burak, S.; Tolga, E.; Omer, T. Does a battery-electric truck make a difference?—Life cycle emissions, costs, and externality analysis of alternative fuel-powered Class 8 heavy-duty trucks in the United States. *J. Clean. Prod.* **2017**, *141*, 110–121. [CrossRef]
7. Seyed, E.H.; Brayden, B. An overview of development and challenges in hydrogen powered vehicles. *Int. J. Green Energy* **2020**, *17*, 13–37. [CrossRef]
8. Fathabadi, H. Fuel cell hybrid electric vehicle (FCHEV): Novel fuel cell/SC hybrid power generation system. *Energy Convers. Manag.* **2018**, *156*, 192–201. [CrossRef]
9. Jamila, S.; Seifeddine, B.E.; Mohamed, B.; Mohamed, F.M. Auto-adaptive filtering-based energy management strategy for fuel cell hybrid electric vehicle. *Energies* **2018**, *11*, 2118. [CrossRef]
10. De Novellis, L.; Sorniotti, A.; Gruber, P. Wheel torque distribution criteria for electric vehicles with torque-vectoring differentials. *IEEE Trans. Veh. Technol.* **2014**, *63*, 1593–1602. [CrossRef]
11. Zunyan, H.; Liangfei, X.; Jianqiu, L.; Minggao, O.Y.; Ziyou, S.; Haiyan, H. A reconstructed fuel cell life-prediction model for a fuel cell hybrid city bus. *Energy Convers. Manag.* **2018**, *156*, 723–732. [CrossRef]
12. Nguyen, G.; Sahlin, S.; Andreasen, S.J.; Shaffer, B.; Brouwer, J. Dynamic modeling and experimental investigation of a high temperature PEM fuel cell stack. *Int. J. Hydrog. Energy* **2016**, *41*, 4729–4739. [CrossRef]
13. Onanena, R.; Oukhellou, L.; Candusso, D.; Harel, F.; Hissel, D.; Aknin, P. Fuel cells static and dynamic characterizations as tools for the estimation of their ageing time. *Int. J. Hydrog. Energy* **2011**, 1730–1739. [CrossRef]
14. Guvelioglu, G.H.; Stenger, H.G. Flow rate and humidification effects on a PEM fuel cell performance and operation. *J. Power Sources* **2007**, *163*, 882–891. [CrossRef]
15. Marzougui, H.; Amari, M.; Kadri, A.; Bacha, F.; Ghouili, J. Energy management of fuel cell/battery/ultracapacitor in electrical hybrid vehicle. *Int. J. Hydrog. Energy* **2017**, *42*, 8857–8869. [CrossRef]

16. Jia, J.; Wang, Y.; Han, M.; Cham, Y.T. Dynamic characteristic study of proton exchange membrane fuel cell. In Proceedings of the IEEE International Conference on Sustainable Energy Technologies, Singapore, 24–27 November 2008.

17. Yun, W.; Chaoyang, W. Modeling polymer electrolyte fuel cells with large density and velocity changes. *J. Electrochem. Soc.* **2005**, *152*, A445–A453. [CrossRef]

18. Junbo, J.; Qi, L.; Youyi, W.; Yew, T.C.; Ming, H. Modeling and dynamic characteristic simulation of a proton exchange membrane fuel cell. *IEEE Trans. Energy Convers.* **2009**, *24*, 283–291. [CrossRef]

19. Yanwei, L.; Yunxue, Z.; Ziyue, L.; Kegang, Z.; Jie, Y. Energy management strategy optimization of hybrid energy storage system based on Radau pseudo-spectral method. *Automot. Eng.* **2019**, *6*, 625–633.

20. Fang, Z.; Feng, X.; Cheng, C.; Yulong, S.; Chuanxue, S. Adaptive model predictive control-based energy management for semi-active hybrid energy storage systems on electric vehicle. *Energies* **2017**, *10*, 1063. [CrossRef]

21. Song, C.; Zhou, F.; Xiao, F.; Chang, C.; Shao, Y. Parameter matching of on-board hybrid energy storage system based on convex optimization method. *J. Mech. Eng.* **2017**, *53*, 44–51. [CrossRef]

22. Lei, Z.; Xiaosong, H.; Zhenpo, W.; Fengchuan, S.; Junjun, D.; David, G.D. Multi-objective optimal sizing of hybrid energy storage system for electric vehicle. *IEEE Trans. Veh. Technol.* **2018**, *2*, 1027–1035. [CrossRef]

23. Li, H.; Ravey, A.; N'Diaye, A.; Djerdir, A. A novel equivalent consumption minimization strategy for hybrid electric vehicle powered by fuel cell, battery and supercapacitor. *J. Power Sources* **2018**, *395*, 262–270. [CrossRef]

24. Yonggang, L.; Jie, L.; Zheng, C.; Datong, Q.; Yi, Z. Research on a multi-objective hierarchical prediction energy management strategy for range extended fuel cell vehicles. *J. Power Sources* **2019**, *429*, 55–66. [CrossRef]

25. Pablo, G.; Juan, P.T.; Luis, M.F.; Francisco, J. Control strategies for high-power electric vehicles powered by hydrogen fuel cell, battery and supercapacitor. *Expert Syst. Appl.* **2013**, *40*, 4791–4804. [CrossRef]

26. Liu, Y.; Li, Z.; Lin, Z.; Zhao, K.; Zhu, Y. Multi-objective optimization of energy management strategy on hybrid energy storage system based on Radau pseudospectral method. *IEEE Access* **2019**, *7*, 112483–112493. [CrossRef]

27. Liangfei, X.; Clemens, D.M.; Jianqiu, L.; Minggao, O.Y.; Zunyan, H. Multi-objective component sizing based on optimal energy management strategy of fuel cell electric vehicles. *Appl. Energy* **2015**, *157*, 664–674. [CrossRef]

28. Hu, Z.; Li, J.; Xu, L.; Song, Z.; Fang, C.; Ouyang, M.; Dou, G.; Kou, G. Multi-objective energy management optimization and parameter sizing for proton exchange membrane hybrid fuel cell vehicles. *Energy Convers. Manag.* **2016**, *129*, 108–121. [CrossRef]

29. Fletcher, T.; Thring, B.; Watkinson, M. An energy management strategy to concurrently optimise fuel consumption & PEM fuel cell lifetime in a hybrid vehicle. *Int. J. Hydrog. Energy* **2016**, *41*, 21503–21515. [CrossRef]

30. Chao, S.; Fengchun, S.; Hongwen, H. Investigating adaptive-ECMS with velocity forecast ability for hybrid electric vehicles. *Appl. Energy* **2017**, *185*, 1644–1653. [CrossRef]

31. Hongwen, H.; Rui, X.; Kai, Z.; Zhentong, L. Energy management strategy research on a hybrid power system by hardware-in-loop experiments. *Appl. Energy* **2013**, *112*, 1311–1317. [CrossRef]

32. Yujie, W.; Zhendong, S.; Zonghai, C. Rule-based energy management strategy of a lithium-ion battery, supercapacitor and PEM fuel cell system. *Energy Procedia* **2019**, *158*, 2555–2560. [CrossRef]

33. Yujie, W.; Zhendong, S.; Zonghai, C. Development of energy management system based on a rule-based power distribution strategy for hybrid power sources. *Energy* **2019**, *175*, 1055–1066. [CrossRef]

34. Ahmadi, S.; Bathaee, S.M.T.; Hosseinpour, A.H. Improving fuel economy and performance of a fuel-cell hybrid electric vehicle (fuel-cell, battery, and ultra-capacitor) using optimized energy management strategy. *Energy Convers. Manag.* **2018**, *160*, 74–84. [CrossRef]

35. Jianjun, H.; Yong, Z.; Zhihua, H.; Jun, X. Parameter matching and control strategies of hybrid energy storage system for pure electric vehicle. *China J. Highw. Transp.* **2018**, *31*, 142–150.